International Journal of Engineering and Geosciences
https://dergipark.org.tr/en/pub/ijeg
e-ISSN 2548-0960

Investigation of the capability of multi-GNSS PPP-AR method in detecting permanent displacements

Mert Bezcioglu [1], Tayyib Ucar [1], Cemal Ozer Yigit [*1]

[1]*Gebze Technical University, Department of Geomatics Engineering, Türkiye*

Keywords
Traditional-PPP
PPP-AR
Displacement monitoring
GPS
Galileo

Research Article
DOI: 10.26833/ijeg.1140959

Received:05.09.2022
Revised: 11.10.2022
Accepted:19.10.2022
Published:08.05.2023

Abstract

The traditional-precise point positioning (PPP) technique may provide a positioning as precise as the relative positioning technique in long-term observation durations. However, since it cannot provide high-precision positioning due to ambiguity problem in short-term observations, the interest in the PPP-AR (Ambiguity Resolution) technique has increased. The main purpose of this study is to investigate the performance of traditional-PPP and PPP-AR techniques for monitoring permanent displacements, considering different observation durations based on different satellite combinations. For this purpose, a displacement simulator that can move precisely in one direction and in the horizontal plane over a small distance was used. 6 different displacements were simulated, and all collected GNSS observations were evaluated with traditional-PPP, PPP-AR, and relative methods. Moreover, these methods were examined by considering the Global Positioning System (GPS), European Global Navigation Satellite System (Galileo), and GPS/Galileo satellite combinations. The findings clearly demonstrated the superiority of the PPP-AR technique outperformed the traditional-PPP technique in short-term observation durations and emphasize the contribution of multi-GNSS (Global Navigation Satellite System) combinations to both methods.

1. Introduction

GNSS technology has been widely used in the detection of horizontal and vertical displacement components of surface deformations such as landslides [1-2], earthquakes [3-5], and engineering structures [6-8]. The estimation of the displacements employed the GNSS technique is usually realized using the repeated campaigns or continuous monitoring stations. The permanent deformation of surfaces such as tectonic faults, landslides, volcanoes, and some engineering structures such as dams can be determined by employing repeated campaigns with the GNSS method. Moreover, real-time deformations of structures such as towers, high-rise buildings, long-span suspension bridges can be predicted by obtaining high-rate GNSS observations with the continuous monitoring stations. Furthermore, high-rate continuous monitoring stations can also be utilized in applications such as GNSS-seismology. Although GNSS measurements in static mode provides millimeter level accuracy in long-term observation durations, the accuracy level decreases in short-term due to effects such as satellite geometry and multipath error [9].

The relative positioning method is widely used to detect permanent deformations at millimeter level precision with repeated campaigns. However, it requires at least two GNSS receivers, one of which is outside the deformation zone. In recent years, however, the traditional-PPP technique, which enables centimeter-level positioning precision by using precise orbit/clock products and employing the stand-alone GNSS receiver, has emerged. Therefore, it has become very popular in the scientific world as a very cost-effective technique [10-13]. The effectiveness of the traditional-PPP technique has been proven in many applications such as characterization of seismic waveforms, structural health monitoring, GNSS buoy, precise orbit determination of low orbit satellites and determination of position of moving objects [14-21]. Furthermore, the performance of determining permanent deformations of the traditional-PPP technique has also been examined [22-26].

* **Corresponding Author**
(mbezcioglu@gtu.edu.tr) ORCID ID 0000-0001-7179-8361
(t.ucar2018@gtu.edu.tr) ORCID ID 0000-0002-4070-4024
*(cyigit@gtu.edu.tr) ORCID ID 0000-0002-1942-7667

Cite this article
Bezcioğlu, M., Uçar, T., & Yiğit, C. O. (2023). Investigation of the capability of multi-GNSS PPP-AR method in detecting permanent displacements. International Journal of Engineering and Geosciences, 8(3), 251-261

In the traditional-PPP technique, the observation duration must be long enough for the ambiguity resolution to converge to the integer value [27]. Compared to the traditional-PPP method, the ambiguity parameter is resolved as an integer in the PPP-AR technique, which makes the PPP-AR technique more effective than the traditional-PPP technique, especially in short-term observation durations. Li et al. [28] examined the PPP and PPP-AR techniques in terms of convergence time and position accuracy by evaluating the GPS and BeiDou satellite combinations in static and kinematic mode, and clearly stated the superiority of the multi-GNSS PPP-AR technique over traditional-PPP method. Li et al. [29] compared the multi-GNSS PPP-AR method using GPS, GLONASS, Galileo and BeiDou satellite combinations with the PPP-AR technique obtained with single and dual satellite combinations. They clearly emphasized that the most accurate position information in the East, North and Up components was obtained with the multi-GNSS PPP-AR technique. Geng et al. [30] used triple frequency observations with GPS, BeiDou, Galileo and QZSS satellite systems to examine how fast the ambiguity resolution is resolved with the PPP-AR technique. The results showed that the more satellites included in the triple frequency, the shorter time to obtain the ambiguity as an integer. Katsigianni et al. [31] examined the contribution of only-Galileo, only-GPS and multi-GNSS satellite observations to traditional-PPP and PPP-AR methods in kinematic mode. The findings clearly stated that the accuracy obtained from only-Galileo and only-GPS techniques is at the same level, and multi-GNSS observations increase the accuracy of position information obtained from traditional-PPP and PPP-AR techniques. Psychas et al. [32] examined the effect of different frequency and satellite combinations on position accuracy and ambiguity resolution. The outcomes demonstrated that the increase in the frequency number improves the position accuracy and ambiguity resolution. Bezcioglu et al. [33-34] collected GNSS observations both static and kinematic mode on two different days with a Zodiac boat on Livingston Island on the Antarctic Peninsula, and the GNSS data processed by the traditional-PPP and PPP-AR technique were compared with the relative positioning technique. The results obtained in the study clearly expressed the superiority of the PPP-AR technique over the traditional-PPP method.

Considering the existing literature, it is seen that the positioning performances of traditional-PPP and PPP-AR techniques were investigated. However, the capabilities of both methods in detecting permanent displacements that occur at a point were not comparatively examined by considering different satellite combinations and observation durations. In this contribution, the ability of traditional-PPP and PPP-AR techniques to detect permanent displacements were evaluated for the first time. A displacement simulator that can precisely move in one direction and in the horizontal plane over a small distance was used in the study, and 6 different displacements of 10, 15, 20, 25, 35 and 40 mm were generated. Observation data collected with only-GPS, only-Galileo and GPS/Galileo satellite combinations were evaluated by both traditional-PPP and PPP-AR techniques by considering the 12-, 6-, 4-, 3-, 2.5-, 2-, 1.5-, and 1-hour observation durations. The ability of both methods that allow obtaining position information with a stand-alone GNSS receiver to estimate the simulated permanent displacements, were validated by considering the relative GNSS positioning technique data obtained from 12-hour observations as ground truth. The outline of this paper is as follows: In section 2, the design of the experiment and the data processing strategy are described; the results are presented in section 3, and finally, section 4 concludes the paper.

2. Method

The displacement simulator apparatus used in the study, the collection and processing of GNSS data, and the mathematical model of geocentric to topocentric coordinate transformation are detailed in the following sections.

2.1. The displacement simulator, GNSS data collection and processing

For the purpose of this study, a displacement simulator, which is shown in Figure 1 and has the ability to move in the horizontal plane, was used. The simulator can produce displacement at sub-mm level precision with the help of a screw and the value of displacement is controlled with the help of a digital caliper. Moreover, geodetic devices such as GNSS receiver, total station and reflector can be mounted on the upper part of the simulator.

Linux-based open-source Pride PPP-AR software was used for traditional-PPP and PPP-AR solutions in this study. The detailed mathematical model of traditional-PPP and PPP-AR techniques were described in detail in Atiz et al. [35]. Processing parameters were also given in Table 1. In the PPP-AR and Network-Adjustment evaluations, the ratio values were chosen as 3.0 for the ambiguity resolution [36].

The experiments were carried out on the roof of the Faculty of Economics of Gebze Technical University in November 2021 and lasted for 8 days. GNSS data for all simulated displacement cases were collected at 10° elevation angle in static mode using a Leica GR30 receiver and a Leica CGA60 antenna and recorded at 20 Hz (0.05 sec) sampling rate. Experiments were performed minimum multipath effect. After collecting 24-hour static data for the reference period (initial position), the antenna was moved 10, 15, 20, 25, 35 and 40 mm in successive days using the simulator. Approximately 12 hours of GNSS observations were collected for each simulated displacement cases. In order to evaluate the effect of the observation durations in both traditional-PPP and PPP-AR techniques, the collected observation data were evaluated with Pride PPP-AR software, by considering the 12-, 8-, 6-, 4-, 3-, 2.5-, 2-, 1.5- and 1-hour observation durations.

Furthermore, to examine the effect of different satellite combinations on the traditional-PPP and PPP-AR methods, solutions were also realized with only-GPS, only-Galileo and GPS/Galileo satellite combinations. The examination and verification of the performance of traditional-PPP and PPP-AR techniques under the effect

of different observations durations and different satellite combinations in the detection of permanent displacements were performed with the relative positioning technique. GAMIT/GLOBK software was used for relative positioning method solutions. Network-adjustment solution for relative positioning method was realized by considering BOR1, BUCU, DRAG, DYNG, GANP, GLSV, GRAZ, JOZ2, MAT1, MDVJ, MEDI, POLV, POTS and SOFI GNSS stations. During the 8-day experiments, it rained at some time intervals. Since the simulator apparatus used in the study is made of wood, considering that there may be an expansion in the apparatus due to wetting, the displacements estimated from the relative method were used as reference, not the displacements produced. In other words, for each network adjustment solution, we used the coordinate from H-files generated by GAMIT, the loosely constrained daily solution and considered them as reference. Finally, the coordinates from the relative positioning, traditional-PPP and PPP-AR methods were transformed to the topocentric coordinate system to calculate the point displacement.

Table 1. Processing strategies of GAMIT/GLOBK and Pride PPP-AR

Options	Network Adjustment	Traditional-PPP	PPP-AR
Sampling Rate	30 sec	0.05sec / 20 Hz	0.05sec / 20 Hz
Elevation Mask	10°	10°	10°
Basic Observable	Code+Phase	Code+Phase	Code+Phase
Tropospheric Model	GMF	GPT3+VMF3	GPT3+VMF3
Weighting Model	1/sin(ele)² "ele:elevation"	W = 1, ele > 30° W = 4 sin(ele)², ele < 30°	W = 1, ele > 30° W = 4 sin(ele)², ele < 30°
Ionosphere	Ionosphere-free linear combination	Ionosphere-free linear combination	Ionosphere-free linear combination
Orbit / Clock	IGS	WUHAN	WUHAN
AR Products		-	WUHAN
Satellite Phase Centre Calibration	Corrected (IGS14)	Corrected (IGS14)	Corrected (IGS14)

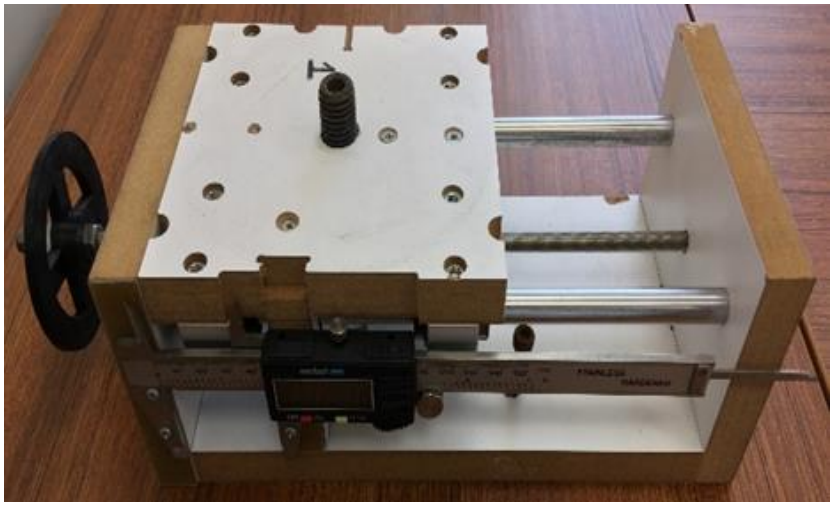

Figure 1. Displacement simulator

2.2. The Coordinate transformation

The GNSS technique provides a position information in the International Terrestrial Reference Frame (ITRF). ITRF is Earth Centered Earth Fixed (ECEF) system, and to calculate the displacement components using the GNSS method, the point coordinates derived from the GNSS technique must be transformed to the local topocentric coordinate system corresponding to the geocentric ITRF system due to the necessity of decomposition of the position and height errors [26]. The common equations between these two systems can be written as Equation 1 and 2.

$$\begin{bmatrix} n_i \\ e_i \\ h_i \end{bmatrix} = R(\varphi_0, \lambda_0) \begin{bmatrix} \Delta x_i \\ \Delta y_i \\ \Delta z_i \end{bmatrix}, \quad \begin{bmatrix} \Delta x_i \\ \Delta y_i \\ \Delta z_i \end{bmatrix} = \begin{bmatrix} x_i - x_0 \\ y_i - y_0 \\ z_i - z_0 \end{bmatrix} \tag{1}$$

$$R(\varphi_0, \lambda_0) = \begin{bmatrix} -sin\varphi_0 cos\lambda_0 & -sin\varphi_0 sin\lambda_0 & cos\varphi_0 \\ -sin\lambda_0 & cos\lambda_0 & 0 \\ cos\varphi_0 cos\lambda_0 & cos\varphi_0 sin\lambda_0 & sin\varphi_0 \end{bmatrix} \tag{2}$$

In Equation 1, x_0, y_0, z_0 $(\varphi_0, \lambda_0, h_0)$ represents the reference point coordinates, and x_i, y_i, z_i is the coordinates obtained from the GNSS technique. $R(\varphi_0, \lambda_0)$ denotes the rotation matrix that provides the transformation from the ITRF coordinate system to the local topocentric coordinate system and is expressed as Equation 2.

The variance-covariance matrix of each solution in the local geodetic system can be calculated using the error propagation formula as shown in Equation 3.

$$R\sum_{n,e,h} = R(\varphi_0, \lambda_0)\sum_{x,y,z} R^T(\varphi_0, \lambda_0) \tag{3}$$

The terms $\sum_{n,e,h}$ and $\sum_{x,y,z}$ in Equation 3 are given in Equation 4.

The displacement of a point can be defined as the statistically significant difference in position between two different periods. For example, assuming that the position of a point P with the covariance matrix $\sum P_t$ at

time t is $P_t(n_t, e_t, h_t)$, and the position of the same point P with the covariance matrix $\sum P_{t+\Delta t}$ at time $t+\Delta t$ is $P_{t+\Delta t}(n_{t+\Delta t}, e_{t+\Delta t}, h_{t+\Delta t})$, the value of the permanent displacement of this point between these two times can be obtained by taking the difference of the coordinates between the times t and $t+\Delta t$ are given in Equation 5.

$$\sum_{n,e,h} = \begin{bmatrix} \sigma_{nn}^2 & \sigma_{ne} & \sigma_{nh} \\ \sigma_{en} & \sigma_{ee}^2 & \sigma_{eh} \\ \sigma_{hn} & \sigma_{he} & \sigma_{hh}^2 \end{bmatrix}, \sum_{x,y,z} = \begin{bmatrix} \sigma_{xx}^2 & \sigma_{xy} & \sigma_{xz} \\ \sigma_{yx} & \sigma_{yy}^2 & \sigma_{yz} \\ \sigma_{zx} & \sigma_{zy} & \sigma_{zz}^2 \end{bmatrix} \quad (4)$$

$$P_{t+\Delta t} - P_t = \begin{bmatrix} \Delta n \\ \Delta e \end{bmatrix} = \begin{bmatrix} n_{t+\Delta t} - n_t \\ e_{t+\Delta t} - e_t \end{bmatrix} \quad (5)$$

As a result, the permanent displacement value of point P between two different times can be calculated as shown in Equation 6.

$$d = \sqrt{\Delta n^2 + \Delta e^2} \quad (6)$$

The covariance matrix of the point coordinates for two different times is given in Equation 7.

$$\sum_{P_t} = \begin{bmatrix} \sigma_{n_t}^2 & \sigma_{n_t e_t} \\ \sigma_{n_t e_t} & \sigma_{e_t}^2 \end{bmatrix} \& \sum_{P_{t+\Delta t}} = \begin{bmatrix} \sigma_{n_{t+\Delta t}}^2 & \sigma_{n_{t+\Delta t e_{t+\Delta t}}} \\ \sigma_{n_{t+\Delta t e_{t+\Delta t}}} & \sigma_{e_{t+\Delta t}}^2 \end{bmatrix} \quad (7)$$

Assuming that the coordinates between the times t and $t+\Delta t$ are uncorrelated, the covariance matrix of the point coordinates is shown in Equation 8.

$$\sum_{P_t P_{t+\Delta t}} = \begin{bmatrix} \sigma_{n_t}^2 & \sigma_{n_t e_t} & 0 & 0 \\ \sigma_{n_t e_t} & \sigma_{e_t}^2 & 0 & 0 \\ 0 & 0 & \sigma_{n_{t+\Delta t}}^2 & \sigma_{n_{t+\Delta t e_{t+\Delta t}}} \\ 0 & 0 & \sigma_{n_{t+\Delta t e_t+\Delta t}} & \sigma_{e_{t+\Delta t}}^2 \end{bmatrix} \quad (8)$$

The variance of the permanent displacement occurring at the point is determined as in Equation 9.

$$\sigma_d^2 = J_d \sum_{P_t P_{t+\Delta t}} J_d^T \quad (9)$$

The Jacobi matrix J_d in Equation 9 is expressed as in Equation 10.

$$J_d = \left[\frac{\delta d}{\delta n_t} \frac{\delta d}{\delta e_t} \frac{\delta d}{\delta n_{t+\Delta t}} \frac{\delta d}{\delta n_{t+\Delta t}} \right] = \left[-\frac{\Delta n}{d} - \frac{\Delta e}{d} \frac{\Delta n}{d} \frac{\Delta e}{d} \right] \quad (10)$$

The standard deviation (σ_d) of the estimated displacement is obtained as follows in Equation 11.

$$\sigma_d = \left(\left(\frac{\Delta n}{d} \right)^2 \left(\sigma_{n_t}^2 + \sigma_{n_{t+\Delta t}}^2 \right) + 2 \frac{\Delta n}{d} \frac{\Delta e}{d} \left(\sigma_{n_t e_t} + \sigma_{n_{t+\Delta t e_t+\Delta t}} \right) + \left(\frac{\Delta e}{d} \right)^2 \left(\sigma_{e_t}^2 + \sigma_{e_{t+\Delta t}}^2 \right) \right)^{1/2} \quad (11)$$

2.3. The Pride PPP-AR Software

Pride PPP-AR, developed by the PRIDE Laboratory at the GNSS Research Center of Wuhan University, is an open-source software that allows to obtain solutions with traditional-PPP and PPP-AR techniques. Pride PPP-AR software has been designed according to the principles of readability, modularity, extensibility, and sustainability. Within the framework of these principles, Pride PPP-AR software is used flexibly and comfortably. Pride PPP-AR supports Linux and Mac OS operating system. It also has a module that works on Windows system. Pride PPP-AR software basically consists of undifferenced processing and ambiguity resolution modules. The undifferenced processing module includes data cleaning and parameter estimations and is responsible for detecting ambiguities in the wide-lane and narrow-lane. Traditional-PPP solutions can be obtained after this stage, and using these ambiguities estimates. The initial ambiguity module then uses phase clock bias products to fix these uncertainties to integer resolution [37].

3. Results

The capability of traditional-PPP and PPP-AR techniques to detect permanent deformations under the effect of different observation durations and different satellite combinations is examined in this part of the contribution. As mentioned in the above sections, the accuracy of traditional-PPP and PPP-AR techniques based on 12-, 8-, 6-, 4-, 3-, 2.5-, 2-, 1.5- and 1-hour GPS, Galileo and GPS/Galileo satellite combinations were investigated employing the relative positioning technique as a reference. Moreover, the superiority of these methods over each other is also discussed.

Table 2 shows the results from both methods discussed in this study, based on 1-hour observations. Table 2 also includes the calculated displacements according to Equation 6 and the standard deviation of the displacements obtained according to Equation 11 for all simulation cases. Furthermore, error column of Table 2 shows how close the permanent displacements obtained from the traditional-PPP and PPP-AR techniques are to the displacements obtained from the relative method. As can be seen from the table, the errors obtained from the PPP-AR technique are quite small compared to the traditional-PPP technique. The differences between the relative method and the traditional-PPP technique range from -13.9 mm to 110.5 mm. Moreover, the differences between the PPP-AR technique and the relative method are between -4.1 mm and 7.5 mm. The average of the errors obtained from the traditional-PPP technique are 21.9 mm, 66.9 mm and 11.6 mm for the only-GPS, only-Galileo and GPS/Galileo satellite combinations, respectively. These differences were obtained as 3.9 mm, 2.3 mm and 2.7 mm for the PPP-AR technique. These results clearly indicate the contribution of multi-satellite combinations to both methods. Furthermore, considering the mean standard deviations obtained from the traditional-PPP technique, the standard deviation of the solutions obtained from the GPS/Galileo satellite combination is 4 times and 2 times smaller, respectively,

than the mean standard deviations derived from the only-GPS-only and only-Galileo solutions. For the PPP-AR technique, on the other hand, the standard deviation values obtained for all satellite combinations are quite similar. These outcomes clearly indicate that the superiority of the PPP-AR technique over the traditional-PPP technique in short-term observation durations.

Table 3 contains results based on 1.5-hour GNSS observations, similar to Table 2. As can be seen from the table, the errors obtained from the PPP-AR technique are also very small at this observation duration compared to the traditional-PPP technique. The differences between the relative method and the traditional-PPP technique are between -7.4 mm and 26 mm, while the differences between the PPP-AR technique and the relative method range from -4.0 mm to 5.7 mm. The mean values of errors derived from the traditional-PPP technique are 4.3 mm, 9.8 mm and 4.4 mm for the only-GPS, only-Galileo and GPS/Galileo satellite combinations, respectively. These differences were obtained as 1.4 mm, 2.7 mm and 1.3 mm for the PPP-AR technique. Also, considering the mean standard deviations from the traditional-PPP technique, similar to the 1-hour measurement time, the standard deviation of the solutions obtained with the GPS/Galileo satellite combination is 4 times and 2 times smaller, respectively, than the mean standard deviations obtained with the GPS-only and Galileo-only solutions. The standard deviation values obtained for all satellite combinations are similar for the PPP-AR technique. Moreover, the mean standard deviation values for only-GPS, only-Galileo and GPS-Galileo satellite combinations are 0.2, 0.2 and 0.1 mm, respectively. These findings clearly demonstrate that the superiority of the PPP-AR technique over the traditional-PPP technique in short observation duration times of 1.5 hours, similar to the 1-hour observations. The main reason for this outcome is that the ambiguity is known as an integer in the PPP-AR technique.

Table 4 represents the results obtained by both methods discussed in the study, based on 2-hour GNSS observations. The errors derived from the PPP-AR technique are smaller than the traditional-PPP technique. The differences between the relative method and the traditional-PPP technique are vary between -1.2 mm and 26.8 mm. These values are range from -5.0 mm to 3.4 mm for the PPP-AR technique. Furthermore, while the mean error value for only-GPS observations in the traditional-PPP technique is 5.3 mm, these values are 14.0 mm and 2.9 mm for only-Galileo and GPS/Galileo satellite combinations, respectively. These values clearly indicate that the contribution of the multi-GNSS combination on both methods. Moreover, as the measurement time increases, the decrease in the error values obtained from the traditional-PPP technique also demonstrate the importance of the observation duration in the traditional-PPP technique. Considering the standard deviations derived from the traditional-PPP technique, the standard deviations of the GPS/Galileo satellite combination are smaller than the derived from the only-GPS and only-Galileo solutions, as in the 1- and 1.5-hour observation durations. The standard deviations of PPP-AR technique, on the other hand, are similar to the prior observation durations. These results clearly revealed that the superiority of the PPP-AR technique over the traditional-PPP technique in 2-hour observation durations.

The results based on different satellite combinations based on 2.5-hour satellite observations are presented in Table 5. From the table, it can be seen that the errors of the Galileo-only satellite observations for the Traditional-PPP technique are 13 times and 9 times higher, respectively, than the errors of the only-GPS and GPS/Galileo satellite combination. Although the differences between the relative method and the traditional-PPP technique range from -5.7 mm to 33 mm, the differences between the PPP-AR technique and the relative method are between -6.0 mm and 3.7 mm. The standard deviation of GPS/Galileo satellite combination for the traditional-PPP technique is smaller than the only-GPS and only-Galileo solutions, and the mean standard deviation values obtained from these satellite combinations are 0.7 mm, 0.4 mm and 0.3 mm, respectively. For PPP-AR technique, the mean standard deviation values are 0.1 mm for all satellite combinations. These results indicate that the PPP-AR technique outperforms the traditional-PPP technique in the 2.5-hour satellite observations, similar to 1-, 1.5- and 2-hour observation durations.

Table 6 contains the results obtained from both methods based on 3-hour GNSS observations. The differences between the relative method and the traditional-PPP technique range from -7.3 mm to 16.5 mm. However, the differences between the PPP-AR technique and the relative method are vary between -5.4 mm and 2.6 mm. Considering the standard deviations obtained from the traditional-PPP technique, it is seen that the average standard deviations obtained from all satellite combinations are comparable to each other, similar to the standard deviations obtained from the PPP-AR technique. These results differ from the prior observations durations, especially considering the traditional-PPP technique based on GPS/Galileo satellite combinations. These results indicate that the necessity of using multi-GNSS satellite observations with a minimum observation duration of 3 hours in estimating permanent displacements employing the traditional-PPP technique.

The results from traditional-PPP and PPP-AR techniques based on 4-hour observation duration are presented in Table 7. As can be seen from the table, the differences between the relative method and the traditional-PPP technique range from -5.0 mm to 11.0 mm. However, the differences between the PPP-AR technique and the relative method are between -32.8 mm and 5.9 mm. Considering that this difference of -32.8 mm is in the value of the first simulated displacement, and the errors obtained from the other cases is vary between -5.1 mm and 5.9 mm, it is clear that this error is an outlier. The average error derived from the GPS/Galileo satellite combination for the traditional-PPP technique is 0.6 mm, also this value is smaller than the errors obtained from the only-GPS and only-Galileo solutions. Moreover, the results of the GPS/Galileo satellite combination performed better as with other observation durations.

The results of both methods discussed in the study based on 6-hour GNSS observations are given in Table 8. With the increase in the observation duration, the errors

obtained from the traditional-PPP technique have decreased considerably. The differences between the traditional-PPP technique and the relative method range from -8.1 mm to 4.5 mm, and the differences between the PPP-AR technique and the relative method are between -7.9 mm and 0.7 mm. The average error values of the only-GPS, only-Galileo, and GPS/Galileo satellite combinations are -1.8 mm, -1.4 mm and -1.9 mm for the traditional-PPP technique, and -3.3 mm, -2.5 mm and -2.7 mm for the PPP-AR technique, respectively. The standard deviations obtained from both methods are similar to each other.

Table 9 shows the results from traditional-PPP and PPP-AR techniques based on 8-hour observation duration. The differences between the relative method and the traditional-PPP technique range from -9.1 mm to 9.5 mm, while the differences between the relative method and the PPP-AR technique are between -9.0 mm and 2.6 mm. Considering the standard deviations derived from both methods, the values obtained from both methods are similar, as in the 4- and 6-hour observation durations.

Table 10 includes outcomes from traditional-PPP and PPP-AR techniques based on 12-hour GNS observations. From the table, it can be seen that the standard deviations of both discussed methods are similar for all satellite combinations. On the other hand, there are slight differences between the estimated permanent displacement derived from the traditional-PPP and PPP-AR techniques and those obtained from the relative method. The differences between the relative method and the traditional-PPP technique range from -9.1 mm to 19.7 mm, while the differences between the PPP-AR technique and the relative method vary between -9.1 mm and 14.4 mm. Although the mean error values are -2.3, 4.6 and 0.4 mm for only-GPS, only-Galileo and GPS-Galileo satellite combinations, respectively, for the traditional-PPP technique, these values are -3.2, 1.00 and 0.0 mm, respectively, for the PPP-AR technique. These results clearly indicate the contribution of multi-satellite combination to the detection of permanent displacements by traditional-PPP and PPP-AR techniques. Furthermore, considering the standard deviation values obtained from both methods, it is clear that both methods are similar in the 12-hour observation duration.

The bar graph of the mean standard deviations of the simulated displacements obtained based on different observation durations and satellite combinations employing the traditional-PPP and PPP-AR techniques is illustrated in Figure 2. As can be seen from the figure, the PPP-AR technique performed better than the traditional-PPP technique for all satellite combinations at observation durations up to 6 hours. The standard deviations obtained from both methods are similar for the 8- and 12-hour observation durations. Considering the mean standard deviation obtained at observation durations up to 6 hours, for only-GPS, only-Galileo, and GPS/Galileo satellite combinations, the PPP-AR technique has, on average, 77.2%, 70.6% and 52.6% smaller standard deviations, respectively, compared to the traditional-PPP technique. For GPS-only observations, the PPP-AR technique has between 55.6% and 90.1% smaller standard deviations than the traditional-PPP technique, 58.7% and 91.2% for Galileo-only observations, and 8.9% and 69.5% for multi-GNSS satellite combinations. These results clearly revealed that the PPP-AR technique is more reliable than the traditional-PPP technique in the determination of permanent displacements at observation durations of 6 hours and less. Moreover, from the Figure 2, it can be seen that the contribution of multi-GNSS satellite combinations for the traditional-PPP technique, especially at short-term observation durations. The multi-GNSS satellite observations improve the standard deviations from only-GPS observations between 7.7% and 82.7%, while it improves the standard deviations from only-Galileo observations between 19.0% and 79.8%. These results clearly demonstrate that the contribution of multi-GNSS observations in short-term observation durations.

Figure 3 represents the differences between the simulated displacements in this contribution and determined employing the relative method and the displacements estimated from the traditional-PPP and PPP-AR techniques, based on different observation durations. From the figure, it can be seen that the PPP-AR technique has slightly smaller error values compared to the traditional-PPP technique, especially at short-term observation durations of up to three hours. In terms of permanent displacement detection applications, the superiority of the PPP-AR technique over the traditional-PPP technique becomes more evident as the observation duration decreases, while the errors of both methods are similar to each other, as the observation time increases. Furthermore, it can be seen that the multi-GNSS observations are in agreement with relative method, especially for observation durations up to 6-hour.

Table 2. Displacements and its statistics obtained from 1-hour GNSS observations employing PPP and PPP-AR methods (RD: Reference Displacement, ED: Estimated Displacement, SD: Standard Deviation, E: Error).

	Traditional-PPP									PPP-AR								
	GPS			Galileo			GPS/Galileo			GPS			Galileo			GPS/Galileo		
RD (mm)	ED (mm)	SD (mm)	E (mm)	ED (mm)	SD (mm)	E (mm)	ED (mm)	SD (mm)	E (mm)	ED (mm)	SD (mm)	E (mm)	ED (mm)	SD (mm)	E (mm)	ED (mm)	SD (mm)	E (mm)
42.5	28.6	1.4	-13.9	116.4	2.1	73.9	47.8	0.4	5.3	38.4	0.1	-4.1	44.8	0.3	2.3	39.5	0.2	-3.1
35.4	23.3	1.8	-12.1	82.9	1.8	47.5	52.6	0.5	17.2	41.4	0.2	6.0	36.5	0.2	1.1	39.1	0.2	3.7
26.7	58.8	1.2	32.1	75.7	1.9	49.0	40.3	0.3	13.6	34.2	0.1	7.5	30.7	0.1	4.0	32.6	0.1	5.9
21.1	44.3	1.1	23.2	114.9	2.9	93.8	39.8	0.2	18.7	24.3	0.1	3.2	22.7	0.1	1.6	23.6	0.0	2.5
16.6	55.5	1.8	38.9	43.5	2.3	26.9	18.6	0.7	2.0	21.1	0.2	4.5	16.9	0.3	0.3	19.3	0.2	2.7
10.8	74.0	2.4	63.2	121.3	2.4	110.5	23.3	0.6	12.5	16.9	0.3	6.1	15.5	0.3	4.7	15.2	0.2	4.4

Table 3. Displacements and its statistics obtained from 1.5-hour GNSS observations employing PPP and PPP-AR methods (RD: Reference Displacement, ED: Estimated Displacement, SD: Standard Deviation, E: Error)

	Traditional-PPP									PPP-AR								
	GPS			Galileo			GPS/Galileo			GPS			Galileo			GPS/Galileo		
RD	ED	SD	E	ED	SD	E	ED	SD	E	ED	SD	E	ED	SD	E	ED	SD	E
(mm)	(mm)	(mm)	(mm)	(mm)	(mm)	(mm)	(mm)	(mm)	(mm)	(mm)	(mm)	(mm)	(mm)	(mm)	(mm)	(mm)	(mm)	(mm)
42.5	35.1	0.4	-7.4	50.2	0.3	7.7	42.9	0.1	0.4	38.2	0.2	-4.4	45.5	0.3	3.0	38.9	0.2	-3.6
35.4	32.2	0.2	-3.2	39.9	0.5	4.5	38.2	0.1	2.8	39.0	0.2	3.6	36.3	0.2	0.9	37.4	0.2	2.0
26.7	38.7	0.3	12.0	34.1	0.5	7.4	34.1	0.1	7.4	31.7	0.1	5.0	30.9	0.1	4.2	31.6	0.1	4.9
21.1	26.1	1.9	5.0	36.1	0.4	15.0	33.0	0.3	11.9	21.4	0.1	0.3	22.5	0.0	1.4	21.8	0.0	0.7
16.6	22.9	0.3	6.3	14.6	0.3	-2.0	15.4	0.1	-1.2	17.6	0.2	1.0	17.6	0.2	1.0	16.9	0.2	0.3
10.8	24.1	2.0	13.3	36.8	1.4	26.0	16.0	0.3	5.2	13.3	0.3	2.5	16.5	0.2	5.7	14.2	0.2	3.4

Table 4. Displacements and its statistics obtained from 2-hour GNSS observations employing PPP and PPP-AR methods (RD: Reference Displacement, ED: Estimated Displacement, SD: Standard Deviation, E: Error)

	Traditional-PPP									PPP-AR								
	GPS			Galileo			GPS/Galileo			GPS			Galileo			GPS/Galileo		
RD	ED	SD	E	ED	SD	E	ED	SD	E	ED	SD	E	ED	SD	E	ED	SD	E
(mm)	(mm)	(mm)	(mm)	(mm)	(mm)	(mm)	(mm)	(mm)	(mm)	(mm)	(mm)	(mm)	(mm)	(mm)	(mm)	(mm)	(mm)	(mm)
42.5	42.0	0.6	-0.5	69.3	0.6	26.8	42.3	0.3	-0.2	37.8	0.2	-4.7	43.7	0.2	1.2	37.5	0.1	-5.0
35.4	41.8	0.6	6.4	42.9	0.5	7.5	40.1	0.3	4.7	38.3	0.2	2.9	36.7	0.1	1.3	37.1	0.1	1.7
26.7	27.2	0.3	0.5	44.4	0.4	17.7	31.3	0.2	4.6	30.2	0.1	3.5	29.2	0.1	2.5	29.9	0.1	3.2
21.1	22.0	1.3	0.9	42.1	0.8	21.0	22.8	0.2	1.7	20.5	0.1	-0.7	21.0	0.1	-0.1	20.7	0.1	-0.4
16.6	16.4	1.2	-0.2	17.7	0.5	1.1	15.5	0.4	-1.2	16.4	0.2	-0.2	15.1	0.1	-1.6	15.6	0.1	-1.0
10.8	35.7	1.1	24.9	20.6	0.9	9.8	18.4	0.5	7.6	14.2	0.2	3.4	13.5	0.2	2.7	14.2	0.2	3.4

Table 5. Displacements and its statistics obtained from 2.5-hour GNSS observations employing PPP and PPP-AR methods (RD: Reference Displacement, ED: Estimated Displacement, SD: Standard Deviation, E: Error)

	Traditional-PPP									PPP-AR								
	GPS			Galileo			GPS/Galileo			GPS			Galileo			GPS/Galileo		
RD	ED	SD	E	ED	SD	E	ED	SD	E	ED	SD	E	ED	SD	E	ED	SD	E
(mm)	(mm)	(mm)	(mm)	(mm)	(mm)	(mm)	(mm)	(mm)	(mm)	(mm)	(mm)	(mm)	(mm)	(mm)	(mm)	(mm)	(mm)	(mm)
42.5	36.9	0.6	-5.7	75.1	0.5	32.6	43.1	0.3	0.6	37.4	0.1	-5.1	41.6	0.2	-0.9	36.6	0.2	-5.9
35.4	47.0	0.6	11.6	43.8	0.3	8.4	36.7	0.3	1.3	38.2	0.1	2.8	34.9	0.2	-0.5	36.5	0.1	1.1
26.7	23.9	0.4	-2.8	44.7	0.4	18.0	27.7	0.3	1.0	28.9	0.1	2.2	27.2	0.1	0.5	27.8	0.1	1.1
21.1	15.9	0.8	-5.2	32.2	0.4	11.1	19.2	0.2	-1.9	19.7	0.1	-1.4	19.4	0.1	-1.7	19.5	0.0	-1.6
16.6	15.0	0.8	-1.6	13.7	0.3	-2.9	15.5	0.3	-1.1	16.3	0.1	-0.3	14.1	0.2	-2.5	14.7	0.1	-1.9
10.8	20.0	0.9	9.2	18.0	0.8	7.2	18.9	0.4	8.1	14.5	0.2	3.7	13.2	0.2	2.4	14.4	0.2	3.6

Table 6. Displacements and its statistics obtained from 3-hour GNSS observations employing PPP and PPP-AR methods (RD: Reference Displacement, ED: Estimated Displacement, SD: Standard Deviation, E: Error)

	Traditional-PPP									PPP-AR								
	GPS			Galileo			GPS/Galileo			GPS			Galileo			GPS/Galileo		
RD	ED	SD	E	ED	SD	E	ED	SD	E	ED	SD	E	ED	SD	E	ED	SD	E
(mm)	(mm)	(mm)	(mm)	(mm)	(mm)	(mm)	(mm)	(mm)	(mm)	(mm)	(mm)	(mm)	(mm)	(mm)	(mm)	(mm)	(mm)	(mm)
42.5	35.2	0.5	-7.3	59.0	0.1	16.5	40.7	0.3	-1.8	37.5	0.1	-5.0	39.8	0.2	-2.7	37.1	0.1	-5.4
35.4	47.1	0.5	11.7	40.4	0.4	5.0	36.8	0.3	1.4	37.2	0.1	1.8	35.1	0.2	-0.3	36.1	0.1	0.7
26.7	28.5	0.5	1.8	36.2	0.3	9.5	27.6	0.3	0.9	27.3	0.0	0.6	26.5	0.1	-0.2	26.7	0.1	-0.1
21.1	16.1	0.4	-5.1	26.3	0.3	5.2	17.8	0.3	-3.4	18.2	0.1	-2.9	18.3	0.1	-2.8	17.7	0.1	-3.4
16.6	14.1	0.0	-2.5	11.4	0.4	-5.2	12.9	0.3	-3.7	14.4	0.1	-2.2	13.3	0.2	-3.3	13.2	0.1	-3.4
10.8	10.3	0.7	-0.5	13.9	0.6	3.1	13.3	0.3	2.5	13.0	0.1	2.2	13.4	0.2	2.6	12.8	0.1	2.0

Table 7. Displacements and its statistics obtained from 4-hour GNSS observations employing PPP and PPP-AR methods (RD: Reference Displacement, ED: Estimated Displacement, SD: Standard Deviation, E: Error)

	Traditional-PPP									PPP-AR								
	GPS			Galileo			GPS/Galileo			GPS			Galileo			GPS/Galileo		
RD	ED	SD	E	ED	SD	E	ED	SD	E	ED	SD	E	ED	SD	E	ED	SD	E
(mm)	(mm)	(mm)	(mm)	(mm)	(mm)	(mm)	(mm)	(mm)	(mm)	(mm)	(mm)	(mm)	(mm)	(mm)	(mm)	(mm)	(mm)	(mm)
42.5	46.6	0.4	4.1	42.6	0.3	0.1	45.0	0.3	2.5	9.7	0.1	-32.8	40.1	0.1	-2.4	40.0	0.1	-2.5
35.4	46.0	0.4	10.6	36.1	0.3	0.7	39.1	0.2	3.7	37.0	0.1	1.6	41.3	0.1	5.9	37.0	0.1	1.6
26.7	31.6	0.4	4.9	27.0	0.3	0.3	28.0	0.2	1.3	26.5	0.1	-0.2	25.6	0.1	-1.1	26.5	0.1	-0.2
21.1	18.6	0.4	-2.5	18.0	0.3	-3.1	17.7	0.2	-3.4	16.2	0.1	-4.9	17.0	0.1	-4.2	16.2	0.1	-4.9
16.6	14.5	0.3	-2.1	11.6	0.4	-5.0	11.4	0.1	-5.2	12.5	0.1	-4.1	11.5	0.1	-5.1	12.5	0.1	-4.1
10.8	7.5	0.4	-3.3	5.6	0.5	-5.2	8.4	0.3	-2.4	10.6	0.2	-0.2	11.4	0.1	0.6	10.6	0.2	-0.2

Table 8. Displacements and its statistics obtained from 6-hour GNSS observations employing PPP and PPP-AR methods (RD: Reference Displacement, ED: Estimated Displacement, SD: Standard Deviation, E: Error)

	Traditional-PPP									PPP-AR								
	GPS			Galileo			GPS/Galileo			GPS			Galileo			GPS/Galileo		
RD (mm)	ED (mm)	SD (mm)	E (mm)	ED (mm)	SD (mm)	E (mm)	ED (mm)	SD (mm)	E (mm)	ED (mm)	SD (mm)	E (mm)	ED (mm)	SD (mm)	E (mm)	ED (mm)	SD (mm)	E (mm)
42.5	45.3	0.2	2.8	46.6	0.2	4.1	45.0	0.2	2.5	40.7	0.1	-1.8	41.8	0.1	-0.7	42.5	0.1	0.0
35.4	39.9	0.2	4.5	34.2	0.2	-1.2	37.7	0.2	2.3	35.6	0.1	0.2	35.7	0.1	0.3	36.1	0.1	0.7
26.7	26.5	0.2	-0.2	27.5	0.2	0.8	26.4	0.2	-0.3	25.5	0.1	-1.2	25.8	0.1	-1.0	25.9	0.1	-0.8
21.1	14.2	0.2	-6.9	18.0	0.3	-3.1	15.3	0.2	-5.8	14.4	0.1	-6.7	16.0	0.1	-5.2	15.0	0.0	-6.1
16.6	8.5	0.1	-8.1	10.7	0.2	-5.9	8.7	0.1	-7.9	8.7	0.1	-7.9	10.3	0.0	-6.3	9.2	0.1	-7.4
10.8	7.8	0.3	-3.0	7.5	0.3	-3.3	8.4	0.2	-2.4	8.7	0.1	-2.1	8.8	0.1	-2.0	8.4	0.1	-2.4

Table 9. Displacements and its statistics obtained from 8-hour GNSS observations employing PPP and PPP-AR methods (RD: Reference Displacement, ED: Estimated Displacement, SD: Standard Deviation, E: Error)

	Traditional-PPP									PPP-AR								
	GPS			Galileo			GPS/Galileo			GPS			Galileo			GPS/Galileo		
RD (mm)	ED (mm)	SD (mm)	E (mm)	ED (mm)	SD (mm)	E (mm)	ED (mm)	SD (mm)	E (mm)	ED (mm)	SD (mm)	E (mm)	ED (mm)	SD (mm)	E (mm)	ED (mm)	SD (mm)	E (mm)
42.5	47.6	0.1	5.1	52.0	0.3	9.5	48.4	0.2	5.9	42.5	0.1	0.0	44.0	0.1	1.5	44.3	0.1	1.8
35.4	40.8	0.1	5.4	38.3	0.2	2.9	39.7	0.2	4.3	37.5	0.1	2.1	36.6	0.1	1.2	38.0	0.1	2.6
26.7	27.5	0.1	0.8	30.7	0.2	4.0	28.4	0.2	1.7	26.6	0.1	-0.1	29.1	0.1	2.4	27.7	0.1	1.0
21.1	12.0	0.0	-9.1	21.3	0.2	0.2	14.1	0.2	-7.0	13.4	0.0	-7.7	19.1	0.1	-2.0	15.3	0.1	-5.8
16.6	8.0	0.1	-8.6	11.7	0.3	-4.9	8.9	0.2	-7.7	7.6	0.0	-9.0	11.6	0.1	-5.0	9.2	0.1	-7.4
10.8	3.4	0.2	-7.4	2.7	0.3	-8.1	3.6	0.2	-7.2	4.6	0.1	-6.2	5.3	0.1	-5.5	4.6	0.1	-6.2

Table 10. Displacements and its statistics obtained from 12-hour GNSS observations employing PPP and PPP-AR methods (RD: Reference Displacement, ED: Estimated Displacement, SD: Standard Deviation, E: Error)

	Traditional-PPP									PPP-AR								
	GPS			Galileo			GPS/Galileo			GPS			Galileo			GPS/Galileo		
RD (mm)	ED (mm)	SD (mm)	E (mm)	ED (mm)	SD (mm)	E (mm)	ED (mm)	SD (mm)	E (mm)	ED (mm)	SD (mm)	E (mm)	ED (mm)	SD (mm)	E (mm)	ED (mm)	SD (mm)	E (mm)
42.5	46.3	0.2	3.8	62.2	0.2	19.7	49.2	0.2	6.7	42.9	0.1	0.4	56.9	0.2	14.4	49.1	0.2	6.6
35.4	39.2	0.2	3.8	39.7	0.1	4.3	39.9	0.1	4.5	37.0	0.1	1.6	37.0	0.1	1.6	37.3	0.1	1.9
26.7	27.4	0.2	0.7	32.6	0.4	5.9	31.0	0.2	4.3	26.1	0.1	-0.6	28.4	0.1	1.7	30.9	0.2	4.2
21.1	13.3	0.1	-7.8	23.3	0.4	2.2	19.4	0.1	-1.7	14.3	0.1	-6.8	20.7	0.2	-0.4	19.4	0.1	-1.7
16.6	7.4	0.1	-9.2	19.6	0.4	3.0	10.9	0.2	-5.7	7.5	0.0	-9.1	15.2	0.2	-1.4	10.7	0.0	-6.0
10.8	5.9	0.1	-4.9	3.6	0.1	-7.3	5.1	0.1	-5.7	6.1	0.0	-4.7	5.7	0.1	-5.1	6.0	0.0	-4.8

Figure 2. Average standard deviation of estimated displacements based on observation durations and satellite combinations for both methods

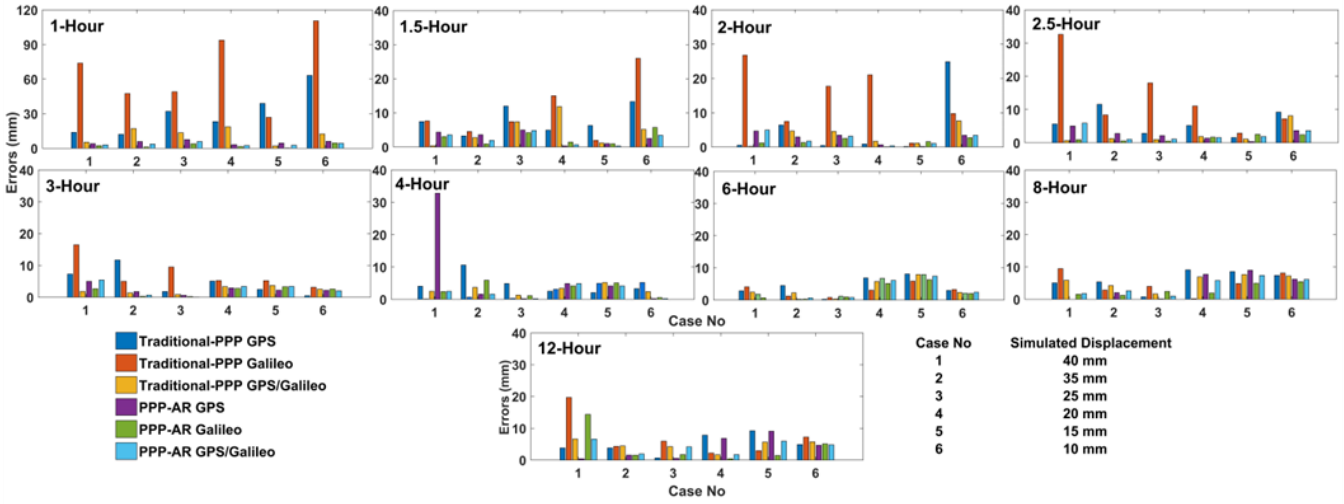

Figure 3. Differences between estimated displacements employing the relative method and displacements obtained from traditional-PPP and PPP-AR techniques based on different observation durations.

4. Conclusion

This study evaluates the capability of traditional-PPP and PPP-AR techniques to detect permanent displacements, by considering the different satellite combinations and observation durations. The results obtained by both methods based on 12-, 6-, 4-, 3-, 2.5-, 2-, 1.5- and 1-hour GNSS observations and the only-GPS, only-Galileo and GPS/Galileo satellite combinations were examined by considering the relative GNSS positioning technique as reference. To investigate the performance of both methods in determining permanent displacements, 6 different permanent displacements of 10, 15, 20, 25, 35 and 40 mm were generated by using a displacement simulator capable of moving in one direction and in the horizontal plane. Considering the mean standard deviation values obtained in the study, the PPP-AR technique for only-GPS, only-Galileo and GPS/Galileo satellite combinations outperformed the traditional-PPP technique on average by 77.2%, 70.6% and 52.6%, respectively. For both methods, the multi-GNSS technique, on the other hand, improves the standard deviations obtained from only-GPS observations by 51.4% on average, while it improves the standard deviations derived from only-Galileo observations by 45% on average. While these results clearly demonstrated the superiority of the PPP-AR technique over the traditional-PPP technique, especially in short observation durations, they also revealed that the multi-GNSS observations improve the results obtained, compared to single-system. It is worth about mentioning that some biases may come from GAMIT solutions, therefore, the displacements error obtained from traditional-PPP and PPP-AR may also include some biases. The findings of the study confirm the contribution of multi-GNSS to the traditional-PPP and PPP-AR methods, similar to previous studies. The outcomes also show the superiority of the PPP-AR technique over the traditional-PPP technique, especially in short-time observation durations, and differ from previous studies in this regard. However, as the observation duration increases, it is worth noting that the traditional-PPP and PPP-AR techniques are similar and comparable to each other.

Acknowledgement

The authors acknowledgement Assoc. Prof. Zeki Coşkun, who passed away in 2015, for the production of the simulation apparatus, and would like to thanks Baris Karadeniz for his field work during the experiments.

Author contributions

Mert Bezcioglu: Analyses, Methodology, Writing-Reviewing and Editing. **Tayyip Ucar:** Data curation, Analyses, Writing-Original draft preparation, Validation, Field study. **Cemal Ozer Yigit:** Supervision, Methodology, Writing-Reviewing and Editing.

Conflicts of interest

The authors declare no conflicts of interest.

References

1. Hastaoglu, K. O., & Sanli, D. U. (2011). Monitoring Koyulhisar landslide using rapid static GPS: a strategy to remove biases from vertical velocities. *Natural hazards*, *58*, 1275-1294.
2. Malet, J. P., Maquaire, O., & Calais, E. (2002). The use of Global Positioning System techniques for the continuous monitoring of landslides: application to the Super-Sauze earthflow (Alpes-de-Haute-Provence, France). *Geomorphology*, *43*(1-2), 33-54.
3. Erdoğan, S., Şahin, M., Tiryakioğlu, İ., Gülal, E., & Telli, A. K. (2009). GPS velocity and strain rate fields in Southwest Anatolia from repeated GPS measurements. *Sensors*, *9*(3), 2017-2034.
4. Hager, B. H., King, R. W., & Murray, M. H. (1991). Measurement of crustal deformation using the Global Positioning System. *Annual Review of Earth and Planetary Sciences*, *19*(1), 351-382.

5. Tiryakioğlu, I. (2015). Geodetic aspects of the 19 May 2011 Simav earthquake in Turkey. *Geomatics, Natural Hazards and Risk*, *6*(1), 76-89.
6. Celebi, M. (2000). GPS in dynamic monitoring of long-period structures. *Soil Dynamics and Earthquake Engineering*, *20*(5-8), 477-483.
7. Lovse, J. W., Teskey, W. F., Lachapelle, G., & Cannon, M. E. (1995). Dynamic deformation monitoring of tall structure using GPS technology. *Journal of surveying engineering*, *121*(1), 35-40.
8. Moschas, F., & Stiros, S. (2011). Measurement of the dynamic displacements and of the modal frequencies of a short-span pedestrian bridge using GPS and an accelerometer. *Engineering structures*, *33*(1), 10-17.
9. Genrich, J. F., & Bock, Y. (1992). Rapid resolution of crustal motion at short ranges with the Global Positioning System. *Journal of Geophysical Research: Solid Earth*, *97*(B3), 3261-3269.
10. Bulbul, S., Bilgen, B., & Inal, C. (2021). The performance assessment of Precise Point Positioning (PPP) under various observation conditions. *Measurement*, *171*, 108780.
11. Kouba, J., & Héroux, P. (2001). GPS precise point positioning using IGS orbit products. *GPS solutions*, *5*(2), 12-28.
12. Li, T., Wang, J., & Laurichesse, D. (2014). Modeling and quality control for reliable precise point positioning integer ambiguity resolution with GNSS modernization. *GPS solutions*, *18*, 429-442.
13. Zumberge, J. F., Heflin, M. B., Jefferson, D. C., Watkins, M. M., & Webb, F. H. (1997). Precise point positioning for the efficient and robust analysis of GPS data from large networks. *Journal of geophysical research: solid earth*, *102*(B3), 5005-5017.
14. Alçay, S., & Atiz, Ö. (2021). Farklı yazılımlar kullanılarak gerçek zamanlı hassas nokta konum belirleme (RT-PPP) yönteminin performansının incelenmesi. *Geomatik*, *6*(1), 77-83.
15. İnyurt, S., & Ulukavak, M. (2020). Web tabanlı GNSS Yazılımlarının (CSRS-PPP, Trimble-RTX) Performansının Araştırılması. *Geomatik*, *5*(2), 120-126.
16. Uçarlı, A. C., Demir, F., Erol, S., & Alkan, R. M. (2021). Farklı GNSS uydu sistemlerinin hassas nokta konumlama (PPP) tekniğinin performansına etkisinin incelenmesi. *Geomatik*, *6*(3), 247-258.
17. Pırtı, A., & Yazıcı, D. (2022). İnternet tabanlı GNSS yazılımlarının doğruluk açısından değerlendirilmesi. *Geomatik*, *7*(2), 88-105.
18. Ogutcu, S. (2020). Performance assessment of IGS combined/JPL individual rapid and ultra-rapid products: Consideration of Precise Point Positioning technique. *International Journal of Engineering and Geosciences*, *5*(1), 1-14.
19. Ogutcu, S. (2020). Performance analysis of ambiguity resolution on PPP and relative positioning techniques: consideration of satellite geometry. *International Journal of Engineering and Geosciences*, *5*(2), 73-93.
20. Öğütcü, S., Shakor, A., & Farhan, H. (2022). Investigating the effect of observation interval on GPS, GLONASS, Galileo and BeiDou static PPP. *International Journal of Engineering and Geosciences*, *7*(3), 294-301.
21. Özdemir, E. G. (2022). Bağıl ve mutlak (PPP) konum çözüm yaklaşımı sunan Web-Tabanlı çevrimiçi veri değerlendirme servislerinin farklı gözlem periyotlarındaki performanslarının araştırılması. *Geomatik*, *7*(1), 41-51.
22. Alcay, S., Ogutcu, S., Kalayci, I., & Yigit, C. O. (2019). Displacement monitoring performance of relative positioning and Precise Point Positioning (PPP) methods using simulation apparatus. *Advances in Space Research*, *63*(5), 1697-1707.
23. Aydin, C., Uygur, S. Ö., Cetin, S., Özdemir, A., & Dogan, U. (2019). Ability of GPS PPP in 2D deformation analysis with respect to GPS network solution. *Survey review*, *51*(366), 199-212.
24. Capilla, R. M., Berné, J. L., Martín, A., & Rodrigo, R. (2016). Simulation case study of deformations and landslides using real-time GNSS precise point positioning technique. *Geomatics, Natural Hazards and Risk*, *7*(6), 1856-1873.
25. Farzaneh, S., Safari, A., & Parvazi, K. (2022). Precise estimation of horizontal displacement by combination of multi-GNSS (Galileo and GPS) observations via the LS-VCE method. *Applied Geomatics*, *14*(2), 267-286.
26. Yigit, C. O., Coskun, M. Z., Yavasoglu, H., Arslan, A., & Kalkan, Y. (2016). The potential of GPS Precise Point Positioning method for point displacement monitoring: A case study. *Measurement*, *91*, 398-404.
27. Choy, S., Bisnath, S., & Rizos, C. (2017). Uncovering common misconceptions in GNSS Precise Point Positioning and its future prospect. *GPS solutions*, *21*, 13-22.
28. Pan, L., Xiaohong, Z., & Fei, G. (2017). Ambiguity resolved precise point positioning with GPS and BeiDou. *Journal of geodesy*, *91*, 25-40.
29. Li, X., Li, X., Yuan, Y., Zhang, K., Zhang, X., & Wickert, J. (2018). Multi-GNSS phase delay estimation and PPP ambiguity resolution: GPS, BDS, GLONASS, Galileo. *Journal of geodesy*, *92*, 579-608.
30. Geng, J., Guo, J., Meng, X., & Gao, K. (2020). Speeding up PPP ambiguity resolution using triple-frequency GPS/BeiDou/Galileo/QZSS data. *Journal of Geodesy*, *94*, 1-15.
31. Katsigianni, G., Loyer, S., & Perosanz, F. (2019). Ppp and ppp-ar kinematic post-processed performance of gps-only, galileo-only and multi-gnss. *Remote sensing*, *11*(21), 2477.
32. Psychas, D., Verhagen, S., & Teunissen, P. J. (2020). Precision analysis of partial ambiguity resolution-enabled PPP using multi-GNSS and multi-frequency signals. *Advances in Space Research*, *66*(9), 2075-2093.
33. Bezcioğlu, M., Yiğit, C. Ö., & Bodur, M. N. (2019). Kinematik PPP-AR ve Geleneksel PPP Yöntemlerin Performanslarının Değerlendirilmesi: Antarktika Yarımadası Örneği. *Afyon Kocatepe Üniversitesi Fen ve Mühendislik Bilimleri Dergisi*, *19*(1), 162-169.
34. Bezcioglu, M., Yigit, C. O., & El-Mowafy, A. (2019). Kinematic PPP-AR in Antarctic. *Sea technology*, *60*(2), 20-23.

35. Atiz, O. F., Ogutcu, S., Alcay, S., Li, P., & Bugdayci, I. (2021). Performance investigation of LAMBDA and bootstrapping methods for PPP narrow-lane ambiguity resolution. *Geo-Spatial Information Science*, *24*(4), 604-614.
36. Verhagen, S., & Teunissen, P. J. (2013). The ratio test for future GNSS ambiguity resolution. *GPS solutions*, *17*, 535-548.
37. Geng, J., Chen, X., Pan, Y., Mao, S., Li, C., Zhou, J., & Zhang, K. (2019). PRIDE PPP-AR: an open-source software for GPS PPP ambiguity resolution. *GPS Solutions*, *23*, 1-10.